

Classification: BIOLOGICAL SCIENCES - Biochemistry

A bacterial process for selenium nanosphere assembly

**Charles M. Debieux^a, Elizabeth J. Dridge^{a,1}, Claudia M. Mueller^{a,1}, Peter Splatt^a,
Konrad Paszkiewicz^a, Iona Knight^a, Hannah Florance^a, John Love^a, Richard W.
Titball^a, Richard J. Lewis^b, David J. Richardson^c and Clive S. Butler^{a,2}**

^aBiosciences, College of Life and Environmental Sciences, University of Exeter, Stocker Road, Exeter
EX4 4QD, UK

^bInstitute for Cell and Molecular Biosciences, University of Newcastle, Newcastle upon Tyne NE2
4HH, UK

^cSchool of Biological Sciences, University of East Anglia, Norwich NR4 7TJ, UK

¹EJD and CMM contributed equally to this work

²To whom correspondence should be addressed at: Biosciences, Centre for Biocatalysis, College of
Life and Environmental Sciences, University of Exeter, Stocker Road, Exeter, UK. EX4 4QD. Fax:
+44 1392 263434; E-mail: c.s.butler@exeter.ac.uk

Abstract

During selenate respiration by *Thauera selenatis* the reduction of selenate results in the formation of intracellular selenium (Se) deposits that are ultimately secreted as Se-nanospheres of ~150 nm in diameter. We report that the Se-nanospheres are associated with a protein of approximately 95 kDa. Subsequent experiments to investigate the expression and secretion profile of this protein have demonstrated that it is up-regulated and secreted in response to increasing selenite concentrations. The protein was purified from Se-nanospheres and peptide fragments from a tryptic-digest were used to identify the gene in the draft *T. selenatis* genome. A matched open reading frame was located encoding a novel protein with a calculated mass of 94.5 kDa. N-terminal sequence analysis of the mature protein revealed no cleavable signal peptide, suggesting that the protein is exported directly from the cytoplasm. The protein has been called Se-factor A (SefA) and homologues of known function have not been reported previously. The *sefA* gene was cloned and expressed in *Escherichia coli* and the recombinant His-tagged SefA purified. *In vivo* experiments demonstrate that SefA forms larger (~300 nm) Se-nanospheres in *E. coli* when treated with selenite and these are retained within the cell. *In vitro* assays demonstrate that the formation of Se-nanospheres upon the reduction of selenite by glutathione are stabilised by the presence of SefA. The role of SefA in selenium nanosphere assembly has potential for exploitation in bio-nanomaterial fabrication.

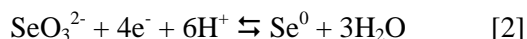
The utilisation of oxygen or nitrogen oxyanions (nitrate and nitrite) as respiratory substrates presents a fortuitous advantage to organisms, since their respiratory products are either aqueous or gaseous and simply diffuse away from the cell. However, this is not always the case. Some micro-organisms that live in niche environments have adapted to utilise more unusual substrates for energy conservation, such as metal ions or chalcogen oxides (1). Often the reduction of these compounds can result in the precipitation of insoluble products that ultimately accumulate within the cell (2). If such compounds are to be used as respiratory substrates, mechanisms for the disposal of the insoluble products are essential. A number of systems exist in Gram-negative bacteria for secretion out of the cell and are commonly referred to as the type 1-6 secretion systems (TxSS¹). A further mechanism for secretion of both soluble and insoluble material is the process of outer membrane vesiculation. In response to stress, a section of the outer membrane forms a distinct spherical vesicle, composed of a lipid bilayer and encloses material exclusively from the periplasm (3, 4).

In the present work, the process of bacterial selenate (SeO₄²⁻) respiration has been used to investigate the mechanism of Se precipitation and secretion. The reduction of selenate follows a sequential series of

Author contributions: CMD, RJL, DJR and CSB designed the research programme. CMD, CMM, EJD, IK, PS, HF and CSB performed the research. HF and KP contributed to analytic tools. CSB, JL, RWT and DJR analysed data. CSB conceived and wrote the paper.

Abbreviations: GSH, glutathione; PMF, proton-motive force; QCR, quinol-cytochrome *c* oxidoreductase; SAM, S-adenosyl-L-methionine; Se⁰, elemental selenium; SefA, selenium factor A; Ser, periplasmic selenate reductase; TAT, twin-arginine translocation; TxSS, type 1-6 secretion systems.

reductive steps ultimately leading to the generation of elemental selenium (Se⁰). Eq.1 and 2 summarise the overall reactions:



Thauera selenatis (a β -proteobacterium) is by far the best studied selenate respiring bacterium (5-8). The selenate reductase (SerABC) isolated from *T. selenatis* (6) is a soluble periplasmic enzyme. The enzyme is a type II molybdoenzyme that comprises three subunits, SerA (96 kDa), SerB (40 kDa) and SerC (23 kDa) and co-ordinates molybdenum, heme (*b*-type) and numerous [Fe-S] centres as prosthetic constituents (9). SerABC contributes to proton-motive force (PMF) generation by accepting electrons from a di-heme *c*-type cytochrome (cyt_{c4}), which mediates electron flux from either a quinol-cytochrome *c* oxidoreductase (QCR) or quinol dehydrogenase (QDH). The use of QCR ensures that selenate reduction is coupled to the Q-cycle mechanism providing a minimum net gain of $2q^+/2e^-$ of proton electrochemical gradient (10).

The resultant product from SerABC is selenite (SeO₃²⁻). The reduction of selenite in *T. selenatis* does not support growth and is not a respiratory substrate. There has been much debate regarding the mechanisms by which selenite is reduced to selenium in bacterial cells. Early reports by Macy and co-workers (11) implicated a nitrite reductase in the process of selenite reduction, by virtue that a non-specific mutant strain of *T. selenatis*, which was deficient in nitrite reductase activity, also failed to produce detectable Se⁰ upon growth in selenate rich medium. The authors speculated that it was probably a periplasmic nitrite reductase that was responsible for selenite reduction. Selenite reacts readily with thiols following the reactions described by Painter (12). Glutathione (GSH) is the primary reduced thiol in *Escherichia coli* and it is now widely believed that it is the prime candidate for bacterial intracellular selenite reduction. Bacteria belonging to the α , β and γ groups of the proteobacteria are all abundant in GSH (13), so the utilisation of GSH for the reduction of selenite during selenate respiration would seem plausible. Selenite reacts readily with GSH producing selenodiglutathione (GS-Se-SG). GS-Se-SG is a good substrate for glutathione reductase and is subsequently reduced to form a selenopersulfide of glutathione (GS-Se⁻). GS-Se⁻ is unstable and dismutates into elemental Se (Se⁰) and reduced GSH. The reaction has been studied for the phototrophic α -proteobacterium, *Rhodospirillum rubrum*, where the reduction of selenite by GSH results in the accumulation of Se particles in the cytoplasm (13). Selenite can also be detoxified by methylation, liberating volatile selenium compounds dimethylselenide and dimethyldiselenide (14, 15). Recently the S-adenosyl-L-methionine (SAM) dependent methyltransferase (TehB) from *E. coli*, which is involved in tellurite resistance, has been shown to be effective in selenium methylation *in vitro* (16). It is therefore of interest to investigate the mechanisms by which selenite is detoxified in a true selenate respiring organism. If *T. selenatis* utilises an intracellular reductant to detoxify selenite during selenate respiration, then elemental Se would inevitably accumulate within the cell. Consequently, it is considered likely that an export system is

required for the secretion of the Se^0 deposits in order to sustain the use of selenate as the sole respiratory substrate. The aim of the present work was to resolve the mechanism by which *T. selenatis* deposits Se during selenate respiration and has led to the discovery of a novel Se-nanosphere assembly protein.

Results

***T. selenatis* secretes selenium nanospheres during selenate respiration.** When *T. selenatis* was grown anaerobically using acetate as the carbon substrate and selenate as the sole electron acceptor, growth was accompanied by the formation of a red precipitate as the culture entered stationary phase. Cell samples were taken at time points selected to represent mid exponential phase (t_1 and t_2), late exponential phase (t_3 and t_4) and early (t_5) and late (t_6) stationary phase (Fig 1A). Samples were analysed using transmission electron microscopy (TEM) (Fig 1B; Fig. S1). Cells entering late exponential growth phase (t_4) appear to start to accumulate electron-dense Se particles within the cytoplasmic compartment (Fig 1B). The particles appear spherical and are approximately 150 nm in diameter, with only one Se-particle per cell. It is also evident that cells during this growth phase start to accumulate granules that appear transparent (Fig 1B), typical of those normally associated with polyhydroxybutyrate, a product known to form in *T. selenatis* when growing using acetate as the carbon substrate (5). As the cells enter stationary phase growth ($t_5 - t_6$), Se particles are observed both inside the cell and in the surrounding medium (Fig. 1B; Fig. S1). No evidence for cell lysis or the accumulation of Se in the periplasmic compartment was obtained. Furthermore, micrographs did not show any evidence of distortion or budding of the outer membrane. Centrifugation of the culture, to remove *T. selenatis* cells and clumps of selenium deposits, liberated a clear supernatant red in colour, which, when analysed by TEM, was shown to contain isolated selenium nanospheres (Fig 1C), uniform electron-dense spheres of ~ 150 nm diameter without a surrounding membrane (Fig 1D).

Secreted protein profile during reduction of selenate and selenite. The spent growth medium containing isolated selenium nanospheres was analysed by SDS-PAGE, to obtain a profile of secreted proteins from *T. selenatis* when grown using selenate as the electron acceptor (Fig. 2A). A single major protein was observed with an apparent molecular mass of ~95 kDa. In order to investigate whether the ~95 kDa protein was secreted in response to selenite, cultures were grown anaerobically using nitrate as the sole electron acceptor in the presence of sodium selenite (10 mM) and, again, the ~95 kDa protein was detected (Fig. 2A). Cultures grown under anaerobic conditions, using nitrate as the electron acceptor, in the absence of selenate/selenite, produced either very little or failed to secrete detectable levels of the ~95 kDa protein. The secretion profile of the ~95 kDa protein was further investigated from cells grown under aerobic conditions in the presence/absence of various oxyanions (Fig. 2B). When *T. selenatis* was grown aerobically on LB medium alone, or in the presence of nitrate, the ~95 kDa protein was not detected. Upon the addition of selenate (10 mM) a faint band was resolved at 95 kDa the amount of which increased when the medium was supplemented with 10 mM selenite. The quantity of protein secreted as a function of time following exposure to selenite was also investigated (Fig. 2C). The amount of the ~95 kDa protein secreted increased

for 16, 24 and 40 h post-incubation with 10 mM selenite. To investigate whether or not a threshold level of selenite concentration was needed to induce secretion of the ~95 kDa protein, aerobic cultures of *T. selenatis* were supplemented with selenite at increasing concentration (0, 0.01, 0.1, 1, 10 mM) and incubated for 24 h. Culture growth was monitored at OD_{600nm} to ensure that the presence of selenite did not have a deleterious effect on cell growth. Red elemental selenium was detected in cultures exposed to > 1mM selenite (Fig. 2D). Analysis of the secreted protein profile shows that the ~95 kDa protein is only detectable from cultures where the selenite concentration was > 1 mM (Fig. 2D). ICP analysis detected selenium in purified protein samples, giving calculated molar ratios of ~320:1 selenium to protein.

Characterisation of the ~95 kDa secreted protein. N-terminal sequencing (Pinnacle Proteomic Facility, Newcastle University) and liquid chromatography/tandem mass spectroscopy of tryptic digest fragments (obtained from both University of York Proteomics Department and Biosciences, University of Exeter) resulted in 124 amino acids of sequence data that was used to identify the gene in the draft assembly of the *T. selenatis* genome (NCBI 53521). Open reading frame (ORF) prediction was carried out using the EMBOSS getorf package (16) and candidate regions were searched via BLAST (BlastX and BlastP) against the non-redundant database of protein sequences. A matched ORF was located on contig 179 and its translation predicted a protein with a calculated mass of 94532.73 Da (Fig. S2). Independent N-terminal sequence analysis of the mature protein produced a peptide sequence (AITATQRT), which aligns adjacent to the start methionine of the target protein identified. The protein does not possess a leader peptide that is cleaved during export from the cell (18-20). Consequently, translocation to the periplasmic compartment directly via a Sec (18) or TAT (19, 20) pathway seems unlikely. Interestingly, 64.3% of the primary sequence is derived from only five amino acids (16.4% Ala; 15.4% Thr; 12% Gly; 10.4% Val; 10.1% Asp). BLAST searches against the NCBI non-redundant database and Swiss-Prot database revealed that there are few statistically significant matches to putative and hypothetical proteins in other microbial organisms. Alignment of SefA with a hypothetical protein (NAL21-3002 (839aa)) identified in the genome of *Nitrosomonas* sp. AL212 (isolated from laboratory activated sludge (21)) reveals another family member (Fig. S2). Other results indicate that similarity to other proteins is limited only to a region covering amino acids 100-200 from the start methionine. One of these was identified in the genome of *Desulfurispirillum indicum* strain S5 (Selin_0231) (22), a known selenate respiring bacterium. Other hits reveal similarity to S-layer proteins, such as SapA from *Campylobacter fetus*. Additional Interpro (23) and PFAM (24) scans of the gene revealed no significant profile hits. Attempts to elucidate gross structure by Hidden-Markov-Model comparison using HHPred (<http://toolkit.lmb.uni-muenchen.de/hhpred>) yielded no additional clues as to the structure and function of the protein, which we have named Se-factor A (SefA). The *sefA* gene sequence has been submitted to NCBI GenBank and is available under accession HQ380173. To determine whether the expression of SefA correlated with the secretion profile observed in the presence of increasing selenite (Fig. 2D), the expression of SefA upon exposure of cells to selenite was evaluated at the mRNA transcription level by RT-PCR and northern blotting (Fig. 2D). Cells grown in the presence of increasing concentrations of

selenite were sampled for mRNA in the stationary phase, just prior to the observation of SefA and Se-nanospheres in the extracellular medium. End-point RT-PCR detected *sefA* transcripts in all samples however, quantitative northern blot analysis revealed that *sefA* was up-regulated in cultures supplemented with 10 mM selenite.

Analysis of the *sefA* loci. Annotation of the ORF's adjacent to SefA (Fig. 3A) revealed that upstream are a putative CHASE2 extracellular sensory domain/guanylate cyclase and a protein containing a tetratricopeptide (TPR) repeat. Downstream is a putative SAM dependent methyltransferase, a further putative peptide and a peptide with a domain of unknown function (DUF). A search for putative transcriptional regulator binding sites upstream of the *sefA* gene was performed using the Prokaryotic Promoter Prediction system (http://bioinformatics.biol.rug.nl/websoftware/ppp/ppp_start.php). This revealed the presence of a putative promoter binding site between positions -87 and -103 relative to the *sefA* gene start site. FNR is a transcriptional regulator active at low oxygen levels. The motif TGTGATTCCCATCACA falls within the Fnr_{Bac}/PrfA Group motifs (TGTGA-N₆-TCACA) classified as Crp/FNR factors by Korner *et al.* (25). Analysis of the intervening region between *sefA* and the putative SAM-dependent methyltransferase cannot identify a known transcriptional regulator binding site. It is thus considered likely that both *sefA* and the gene encoding the putative methyltransferase are in the same operon. Consequently, we have called the methyltransferase SefB. SefB is a 513 aa protein with a calculated molecular weight of 56.9 kDa. PFAM analysis identifies both putative methyltransferase and regulatory domains. A SefB homologue has also been located in *D. indicum* strain S5 (Selin_0233).

Expression of SefA in *E. coli*, *in vivo* localisation and resistance to selenite. The gene encoding SefA was cloned and expressed in *E. coli* (see SI Materials and Methods, Fig. S3). Western blot analysis of soluble cell fractions and extracellular medium are shown in Fig. 4A. After 4 h induction, SefA is detected predominantly in the soluble cell fraction, but is also detectable in the extracellular medium. Analysis of the medium by SDS-PAGE analysis would indicate that this is not due to cell lysis. At 19 h after induction the amount of SefA detected in both fractions has increased substantially. In the presence of selenite (10 mM), SefA is again detected in both the soluble cell fractions and the extracellular medium at both time points. Samples that were not treated with IPTG failed to produce detectable SefA in either fraction. Further analysis of the selenite treated samples by TEM revealed that cells not expressing SefA were shown to accumulate Se particles ranging in size from 30 – 50 nm (Fig. 4B). Cells treated with selenite/IPTG accumulated larger particles (~300 nm) in the cytoplasm (Fig. 4C). No evidence was found for extracellular Se nanospheres. The results show that SefA can be expressed in *E. coli* and indicate it might be substrate for protein export. The addition of selenite to the culture has no obvious effect on the level of exported SefA, suggesting that secretion from *E. coli* is not conditional upon Se binding. These data suggest that whilst apo-SefA can be secreted from *E. coli*, a specific export system is required for Se-nanosphere secretion. Analysis of *E. coli* (pET33b-*sefA*) to selenite resistance, shows that cells in which SefA is expressed are more resistant to selenite concentrations up to 25 mM than those cells without SefA (Fig. 4D).

***In vitro* assembly of selenium nanospheres is facilitated by SefA.** rSefA was purified using immobilized nickel affinity chromatography and gel filtration (Fig. S3). Purified rSefA was analysed by SDS-PAGE and demonstrated a migration position similar to that of the native protein from *T. selenatis* (Fig. S3). The Se particles, as secreted by *T. selenatis* during selenate respiration and once separated by filtration through the 0.2 μ M filter, displayed an absorbance peak at 400 nm when analysed by electron absorption spectroscopy. Consequently, absorbance at 400 nm was used to monitor the formation of Se particles *in vitro* from the reaction of reduced glutathione (4 mM) with selenite (0.5 mM) in the presence or absence of rSefA. Using molar ratios of glutathione:selenite >4:1 ensured that GS-Se-SG was reduced to GSSeH which readily decomposed to Se⁰ (13). Fig. 4E shows formation of selenium particles as a function of time. Under these conditions, the reaction in the absence of SefA proceeded to give a maximum absorbance of approximately 1 unit and produced a distinct black precipitate in the reaction cuvette. In the presence of SefA, the maximum absorbance was stabilized at 0.5 units and the particles remained in solution giving the typical red/orange colour. TEM analysis of the particle formation under the reaction conditions are shown in Fig. 4F and 4G. The black precipitate observed in the absence of SefA was visible under TEM as vitreous Se deposits (Fig 4F). In the presence of SefA distinct Se-nanospheres were observed with sizes ranging from 20-300 nm (Fig 4G).

Discussion

Bacteria that are capable of the respiration of selenium oxyanions have been isolated from a number of selenium rich environments (26, 27). Using selenium oxides as the sole electron acceptor presents the organism with the challenge of what to do with the elemental Se product following the subsequent reductions. For some bacteria that catalyse the reduction of selenate to Se⁰, Se deposits have been observed to accumulate within the cytoplasmic compartment, whilst in others, they are secreted from the cell (28). For example; *Enterobacter cloacae* SLD1a-1 (29), *R. rubrum* (30) and *Desulfovibrio desulfuricans* (31) have all been found to bioreduce selenite to selenium both inside and outside the cell. *E. coli* is also able to reduce selenite forming deposits both in the periplasmic and cytoplasmic compartments (32). However, for a selenate respirer such as *T. selenatis*, a build-up of Se in the cytoplasm or periplasm might not be sustainable and could lead to necrosis. Consequently, mechanisms have evolved for the secretion of solid Se⁰ precipitates. In the present work, the process by which *T. selenatis* deposits Se during selenate respiration has been investigated. A novel secreted protein, SefA, has been identified and homologues of known function have not been reported previously. Evidence is presented that SefA facilitates Se-nanosphere assembly prior to export from the cell.

The observation that SefA has no detectable selenite reductase activity would suggest that SefA functions only to bind to, or to stabilise, Se⁰. Since selenate reduction in *T. selenatis* is periplasmic, the location of the selenite reductive pathway remains unclear. A previous study has suggested that a periplasmic nitrite reductase could be responsible for selenite reduction (11), however, selenite reductase activity in periplasmic

fractions, using reduced methyl viologen as the electron donor, has not been detected. Based upon the present data it is suggested that selenite reduction occurs in the cytoplasm. The reduction to Se^0 could be due to interaction with thiols, possibly GSH, since GSH is abundant in both the β -proteobacteria (*T. selenatis*) and γ -proteobacteria (*E. coli*) (12,13). GSH is synthesized by sequential actions of γ -glutamylcysteine synthetase (GshA) and glutathione synthetase (GshB), and homologues for both GshA and GshB have been identified in the draft *T. selenatis* genome. The reaction of selenite with GSH can result in the generation of O_2^- , which is detoxified in part by cytochrome *c* (13). Interestingly, we have previously identified a *c*-type cytochrome (cytc-Ts7) that is up-regulated during selenate respiration, but is not involved in electron transfer to SerABC (10). It is possible that the function of cytc-Ts7 is to help detoxify any O_2^- generated.

The diagram presented in Fig. 5 shows the model for the selenate respiration pathway in *T. selenatis*. The reduction of selenate draws electrons from the membrane-bound QCR, which concomitantly provides a net gain of $2q^+/2e^-$ of proton electrochemical gradient (10). Whilst the utilisation of a QCR is unusual for a periplasmic molybdoenzyme, the additional 2H^+ translocated via the link to the Q-cycle could provide the driving force for the translocation of selenite across the cytoplasmic membrane. In this case, energy would also need to be conserved by the utilization of an electrogenic primary dehydrogenase. The exact nature of the selenite transporter in *T. selenatis* is unknown, but in *E. coli* it has been suggested that selenite crosses the cytoplasmic membrane via the sulphate transporter (33). Once in the cytoplasm, selenite could be reduced by GSH (or other reductants) and the resultant Se^0 binds to SefA forming a nanosphere inside the cell. In addition, it is likely that the putative SAM-dependent methyltransferase (SefB), downstream from SefA, might function to generate methyl selenite or other volatile selenium compounds. The involvement of the tellurite resistance SAM-dependent methyltransferase (TehB) has been shown recently to be effective in the methylation of both tellurite and selenite (16). Interestingly, whilst *E. coli* TehB has been identified as responsible for the methylation of tellurite *in vitro* (16), *in vivo* assays have not established the production of volatile methylated tellurium, yet precipitation of tellurium within cells is clearly seen as black deposits (34). The identification of SefA and SefB in the same operon, suggests that in *T. selenatis* there could be a link between both reductive and methylation dependent selenite detoxification.

How does the Se-nanosphere get out of the cell? SefA does not have an N-terminal signal sequence for targeting to the periplasmic compartment. Furthermore, analysis of neighbouring genes/proteins on the chromosome does not identify any likely TAT substrate candidates that might “carry” SefA to the periplasm. The size of the particles is consistent with those seen during outer membrane vesiculation (20 - 250 nm) (4), but by TEM we see no evidence of outer membrane distortion or bulging. Furthermore, outer-membrane vesicles contain exclusively material from the periplasm, whereas the Se particles are not associated with other periplasmic proteins (such as SerABC) and from the EM images SefA-Se-nanospheres would appear to be translocated directly from the cytoplasm. Analysis of the *T. selenatis* draft genome assembly using an Interpro scan of all ORFs > 50 amino acids revealed the presence of all but Type V secretion systems. SefA

could thus be exported via the T6SS since other proteins secreted by this system also lack an N-terminal signal sequence and are not first translocated to the periplasmic compartment. S-layer proteins (which show some sequence similarity to SefA) are typically substrates for the T1SS. Most notably, T1SS substrates share a common distinctive glycine rich repeat (GGXGXDXXX) and contain very few or no cysteine residues (35,36), both features of SefA. These characteristics might explain why SefA was detected in the extracellular medium when expressed in *E. coli*. However, it would appear that in *T. selenatis* the SefA-Se complex is assembled in the cell and only exported once at an optimum size. *T. selenatis* is somehow capable of sensing the size of the internal particles and selectively only secretes Se-nanospheres of ~150 nm diameter. Evidently, *E. coli* lacks this capability and accumulated much larger Se-SefA particles, suggesting that the Se-nanosphere export system is specific to *T. selenatis*. The mechanism of how the Se-nanospheres as a whole are assembled and secreted across the inner and outer membranes remains unknown.

The identification of another SefA family member in *Nitrosomonas* sp. (AL212 NAL212_3002) is interesting and deserves comment. The strain AL212 was isolated from cultures that could grow in up to 10.7 mM (NH₄)SO₄, and along with strain JL21 (grew in 3.57 mM) were called the “sensitive” strains (21). It had been noted in previous studies that some of the other strains isolated from treatment plants and laboratory sludges, once enriched in culture with (NH₄)SO₄, showed the formation of “particles” in the cytoplasm (37), but not in strain JL21. Curiously, the EM images of strain JL21 (and to a lesser extent AL212) reported in Suwa *et al.* (21) show evidence of extracellular spherical particles reminiscent of those created by SefA. It would seem likely that in this case, these particles could be based upon the chalcogen sulphur rather than selenium.

Various proteins that bind Se have been reported. Rhodanese (a sulfur transferase) (38), cysteine/selenocysteine lyases (39), SeBP (40) from *Methanococcus vannielii* and the glycolytic enzyme glyceraldehyde-3-phosphate dehydrogenase (GAPDH) (41) can all bind selenium at a reactive cysteine residue. Analysis of the amino acid sequence of SefA reveals no cysteine residues are present, indicating that the Se-SefA interaction is not via a direct thiol ligand. BSA has also been shown to stabilise nano-Se following reduction by GSH. As BSA is (moderately) soluble in salt solutions it serves well as a carrier for molecules of low water solubility. The non-specific interaction with BSA and Se is thought to stabilise the Se-nanosphere by allowing interactions of its functional groups with water and by sterically avoiding Se aggregation in aqueous solution (42), thus capping the particle surface. It would seem likely that, in the absence of any thiol ligands, SefA would also function as a capping agent, providing reaction sites for the creation of Se-nanospheres and providing a shell to prevent aggregation of the secreted particles.

The involvement of SefA in Se-nanosphere assembly might have applications pertinent to nanotechnology. In particular, selenium nanoparticles have excellent bioavailability, high biological activity and relatively low toxicity. A number of methods have been developed to generate Se nanoparticles, nano-rods and nano-wires (43), but most require the use of hydrazine, glycol, surfactant or high temperature. A number of

studies have also taken advantage of biomolecules to generate Se-nanoparticles *in vitro*. For example, Abdelouas *et al.* (44) have used reduced cytochrome *c* to synthesize Se nano-wires at room temperature. More recently, Zhang *et al.* (45) synthesized t-Se nano-wires using β -carotene as an *in situ* soft template. Having identified a novel protein that can stabilise Se-nanospheres secreted from *T. selenatis*, this could, through molecular engineering, enable particles to be produced with structural arrangements that are not only unique, but have yet also to be reproduced by conventional chemical synthesis. The extra-cellular secretion of such nanoparticles from *T. selenatis* also has distinct benefits when compared to those bacterial systems that display intra-cellular accumulation, and as such the current work could present a new opportunity for the synthesis of novel secreted Se-nanomaterials.

Materials and Methods

See Supporting Information (SI Materials and Methods) for details of growth of *T. selenatis*, isolation of SefA, identification of the *sefA* gene, generation of recombinant SefA in *E. coli*, assays for *in vitro* selenium nanosphere formation, imaging *T. selenatis* cells and Se-nanospheres by TEM, RT-PCR and northern blotting reactions and protocols.

We thank Gavin Wakely, Edgar Dawkins and Oluwakemi Obasa for help with preliminary experiments. *Thauera selenatis* was kindly provided by Dr Joanne Santini (University College London). We thank Dr David Studholme (University of Exeter), Dr Ian Henderson (University of Birmingham), Dr Jon Marles-Wright and Dr Elisabeth Lowe (University of Newcastle) for useful discussions and Kevin Brigden (University of Exeter) for preliminary ICP analysis. We also thank Carmen Denman and Dr Alan Brown (University of Exeter) for help with the northern blotting. CMD, EJD and IK were funded by a research grant from the Biotechnology and Biological Sciences Research Council and the Engineering and Physical Sciences Research Council (life science interface) (BB/D00781X/1) to CSB, R JL and DJR.

REFERENCES

1. Richardson DJ (2000) Bacterial respiration: a flexible process for a changing environment. *Microbiology* 146:551-571.
2. Lloyd JR (2003) Microbial reduction of metals and radionuclides. *FEMS Micro rev* 27:411-425.
3. McBroom AJ, Kuehn MJ (2007) Release of outer membrane vesicles by Gram-negative bacteria is a novel envelope stress response. *Mol Microbiol* 63:545-558.
4. Kulp A, Kuehn MJ (2010) Biological functions and biogenesis of secreted bacterial outer membrane vesicles. *Annu Rev Microbiol* 64:163-184.
5. Macy JM, et al. (1993) *Thauera selenatis* gen-nov, sp-nov, a member of the beta-subclass of proteobacteria with a novel type of anaerobic respiration. *Int J Syst Bacteriol* 43:135-142.

6. Schröder I, Rech S, Krafft T, Macy JM (1997) Purification and characterization of the selenate reductase from *Thauera selenatis*. *J Biol Chem* 272:23765-23768.
7. Krafft T, Bowen A, Theis F, Macy JM (2000) Cloning and sequencing of the genes encoding the periplasmic-cytochrome B-containing selenate reductase of *Thauera selenatis*. *DNA Seq* 10:365-377.
8. Maher MJ, et al. (2004) X-ray absorption spectroscopy of selenate reductase. *Inorg Chem* 43:402-404.
9. Dridge EJ, et al. (2007) Investigation of the redox centres of periplasmic selenate reductase from *Thauera selenatis* by EPR spectroscopy. *Biochem J* 408:19-28.
10. Lowe EC, et al. (2010) Quinol-cytochrome *c* oxidoreductase and cytochrome *c4* mediate reelectron transfer during selenate respiration in *Thauera selenatis*. *J Biol Chem* 285:18433-18442.
11. DeMoll-Decker H, Macy JM (1993) The periplasmic nitrite reductase of *Thauera selenatis* may catalyze the reduction of selenite to elemental selenium *Arch Microbiol* 160:241-247.
12. Painter EP, (1941) The chemistry and toxicity of selenium compounds with special reference to the selenium problem. *Chem Rev* 28:179-213.
13. Kessi J, Hanselmann KW (2004) Similarities between the abiotic reduction of selenite with glutathione and the dissimilatory reaction mediated by *Rhodospirillum rubrum* and *Escherichia coli*. *J Biol Chem* 279:50662-50669.
14. Ranjard L, Nazaret S, Cournoyer B (2003) Freshwater bacteria can methylate selenium through thiopurine methyltransferase pathway. *Appl Environ Microbiol* 69:3784-3790.
15. Ranjard L, et al. (2004) Characterization of a novel selenium methyltransferase from freshwater bacteria showing strong similarities with the calicheamicin methyltransferase. *Biochim Biophys Acta* 1679:80-85.
16. Choudhury HG, Cameron AD, Iwata S, Beis K (2011) Structure and mechanism of the chalcogen detoxifying protein TehB from *Escherichia coli*. Doi:1042/BJ20102014.
17. Rice P, Longden I, Bleasby A (2000) EMBOSS: The European Molecular Biology Open Software Suite. *Trends in Genetics* 16: 276-277.
18. Pugsley AP (1993) The complete general secretory pathway in gram-negative bacteria. *Microbiol Mol Biol Rev* 57:50-108.
19. Berks BC, Sargent F, Palmer T (2000) The Tat protein export pathway. *Mol Microbiol* 35:260-274.
20. Sargent F (2007) Constructing the wonders of the bacterial world: biosynthesis of complex enzymes. *Microbiology SGM* 153:633-651.
21. Suwa Y, Sumino T, Noto K (1997) Phylogenetic relationships of activated sludge isolates of ammonia oxidizers with different sensitivities to ammonia sulphate. *J Appl Microbiol* 43:373-379.
22. Rauschenbach I, Narasingarao P, Haggblom M (2011) *Desulfurispirillum indicum* sp. nov., a selenate and selenite respiring bacterium isolated from an estuarine canal in southern India. *Int J Syst Evol Microbiol* 61:654-658.
23. Quevillon E, et al. (2005) InterProScan: protein domains identifier. *Nucleic Acids Res.* 33 (Web Server issue):W116-W120.

24. Finn RD, et al. (2010) The Pfam protein families database *Nucleic Acids Res. Database*
25. Körner H, Sofia HJ, Zumft WG (2003) Phylogeny of the bacterial superfamily of Crp-Fnr transcription regulators: exploiting the metabolic spectrum by controlling alternative gene programs. *FEMS Micro Rev* 27:559-592.
26. Stolz JF, Oremland RS (1999) Bacterial respiration of arsenic and selenium. *FEMS Microbiol Rev* 23: 615-627.
27. Stolz JF, Basu P, Santini JM, Oremland RS (2006) Arsenic and selenium in microbial metabolism. *Annu Rev Microbiol* 60:107-30.
28. Oremland RS, et al. (2004) Structural and spectral features of selenium nanospheres produced by Se-respiring bacteria. *Appl Environ Microbiol* 70:52-60.
29. Losi ME, Frankenberger WT (1997) Reduction of selenium oxyanions by *Enterobacter cloacae* SLD1a-1: Isolation and growth of the bacterium and its expulsion of selenium particles. *Appl Environ Microbiol* 63:3079-3084.
30. Kessi J, Ramuz M, Wehrli E, Spycher M, Bachofen R (1999) Reduction of selenite and detoxification of elemental selenium by the phototrophic bacterium *Rhodospirillum rubrum*. *Appl Environ Microbiol* 65:4734-4740.
31. Tomei FA, et al. (1995) Transformation of selenate and selenite to elemental selenium by *Desulfovibrio desulfuricans*. *J Ind Microbiol* 14:329–336.
32. Gerrard TL, Telford JN, Williams HH (1974) Detection of selenium deposits in *Escherichia coli* by electron microscopy. *J Bacteriol* 119:1057-1060.
33. Turner RJ, Weiner JH, Taylor DE (1998) Selenium metabolism in *Escherichia coli*. *Biometals* 11:223-7.
34. Liu M, et al. (2000) *Escherichia coli* requires S-adenosylmethionine as a cofactor to mediate tellurite resistance. *J Bacteriol* 182:6509-6513.
35. Baumann U, Wu S, Flaherty KM, McKay DB. (1993) Three-dimensional structure of the alkaline protease of *Pseudomonas aeruginosa*: a two-domain protein with a calcium binding parallel beta roll motif. *EMBO J* 1993 12:3357-64.
36. Delepelaire P (2004) Type I secretion in gram-negative bacteria. *Biochim Biophys Acta* 1694:149-161.
37. Suwa Y, Imamura Y, Suzuki T, Tashiro T, Urushigawa Y (1994) Ammonia-oxidizing bacteria with different sensitivities to (NH₄)SO₄ in activated sludges, *Wat Res* 28:1523-1532.
38. Ogasawara Y, Lacourciere GM, Stadtman TC (2001) Formation of a selenium-substituted rhodanese by reaction with selenite and glutathione: Possible role of a protein perselenide in a selenium delivery system. *Proc Natl Acad Sci USA* 98:9494-9498.
39. Mihara H, et al. (1999) A *nifS*-like Gene, *csdB*, Encodes an *Escherichia coli* counterpart of mammalian selenocysteine lyase: gene cloning, purification, characterisation and preliminary X-ray crystallographic studies. *J Biol Chem* 274:14768-14772.
40. Patteson KG, Trivedi N, Stadtman TC (2005) *Methanococcus vannielii* selenium-binding protein (SeBP): Chemical reactivity of recombinant SeBP produced in *Escherichia coli*. *Proc Natl Acad Sci*

USA 102:12029-12034.

41. Lacourciere GM, Levine RL, Stadtman TC (2002) Direct detection of potential selenium delivery proteins by using an *Escherichia coli* strain unable to incorporate selenium from selenite into proteins. *Proc Natl Acad Sci USA* 99:9150-9153.
42. Bücking W, Massadeh S, Merkulov A, Xu S, Nann T (2010) Electrophoretic properties of BSA-coated quantum dots. *Anal Bioanal Chem* 396:1087–1094.
43. Gates B, Mayers B, Cattle B, Xia Y (2002) Synthesis and characterization of uniform nanowires of trigonal selenium. *Adv Funct Mater* 12:219–227.
44. Abdelouas A, et al. (2000) Using cytochrome *c*, to make selenium nanowires. *Chem Mater* 12:1510.
45. Zhang B, et al. (2006) Biomolecule-assisted synthesis of single-crystalline selenium nanowires and nanoribbons via a novel flake-cracking mechanism. *Nanotechnology* 17:385-390.

FIGURE LEGENDS

Fig. 1. Physiological analysis of Se-nanosphere production. (A) Growth curve of *T. selenatis* grown on acetate using selenate (10 mM) as the sole electron acceptor (Error bars are SEM; $n = 10$ cultures). Time points t_1 - t_6 indicate the samples used for EM analysis. (B) TE Micrographs of time points from (A). Micrographs t_1 and t_2 show mid exponential phase; t_3 and t_4 show late exponential phase; t_5 and t_6 show stationary phase. Scale bar = 200 nm. Selenium deposits are indicated by an arrow. Poly- β -hydroxybutyrate granular deposits are indicated by an asterisk. TE micrographs of purified Se-nanospheres. (A) Scale bar = 500 nm. (B) Scale bar = 50 nm.

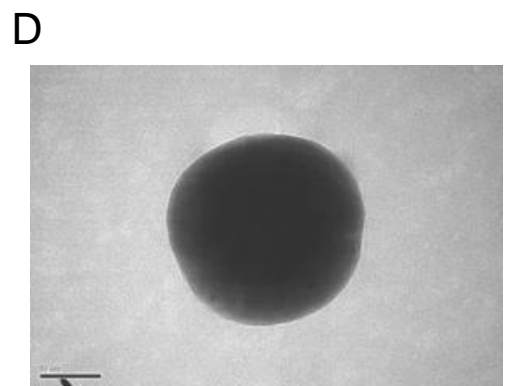
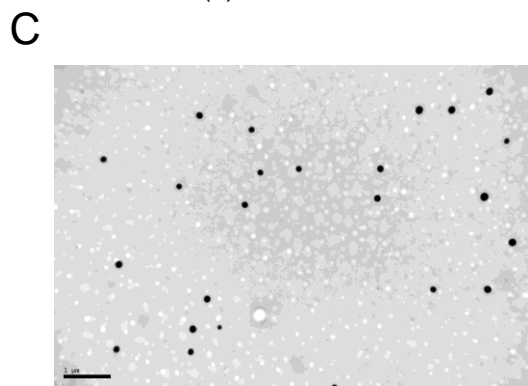
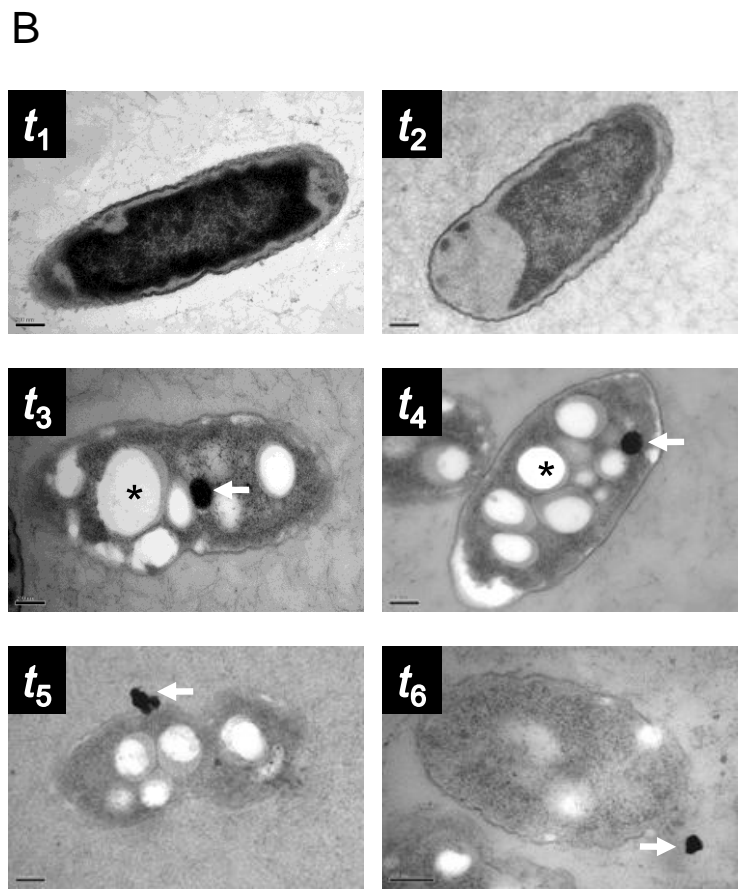
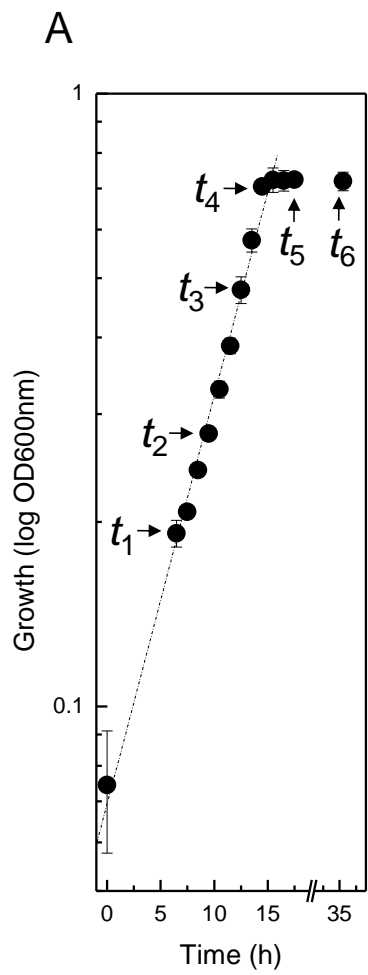
Fig. 2. Protein analysis of Se-nanospheres from *T. selenatis*. (A) SDS-PAGE gels stained for secreted proteins from *T. selenatis* grown under anaerobic conditions. Lane 1, Invitrogen SeeBlue Plus2 Prestained Standard; lane 2 protein from cells grown on selenate (10 mM); lane 3, protein from cells grown on nitrate (10 mM) plus selenite (10 mM); (B) SDS-PAGE gel stained for total protein secreted in the extracellular medium from cells grown aerobically under different growth conditions. Lane 1, Invitrogen SeeBlue Plus2 Prestained Standard; lane 2, control (cells grown in LB medium only); lane 3, LB medium containing 10 mM selenite prior to inoculation with *T. selenatis*; lane 4, cells grown in LB medium supplemented with 10 mM selenate; lane 5, cells grown in LB medium supplemented with 10 mM nitrate; and lane 6, cells grown in LB medium supplemented with 10 mM selenite. (C) Secreted proteins from *T. selenatis* grown under aerobic conditions on LB medium supplemented with selenite (10 mM) following incubation for 16, 24 and 40 h, respectively. (D) Analysis of protein secretion and regulation upon exposure to increasing concentrations of selenite. i) observed selenium precipitation in cultures; ii) SDS-PAGE analysis of secreted proteins; iii) and iv) end-point RT-PCR of *sefA* and 16S transcripts; v) northern blot of *sefA* transcript.

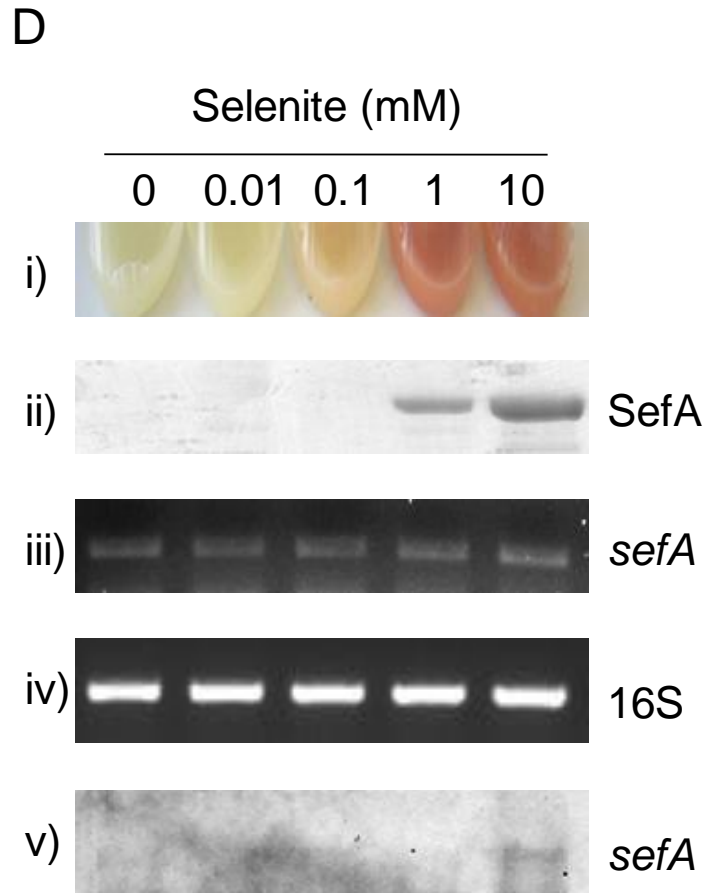
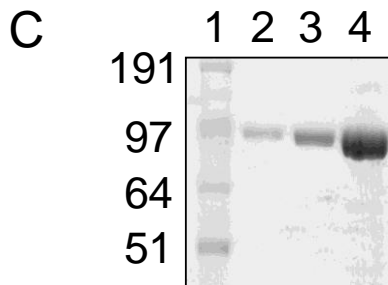
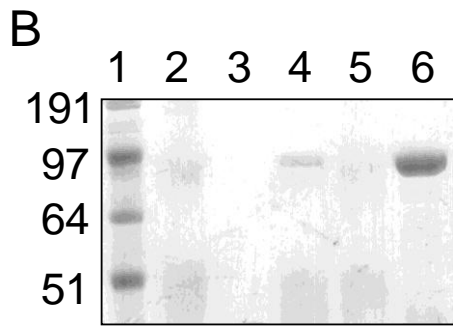
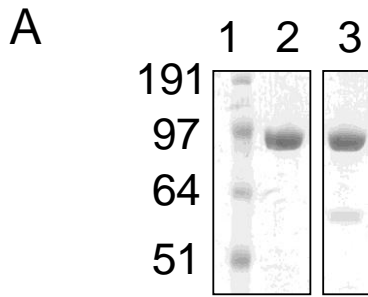
Fig. 3. Analysis of the *sef* operon. (A) Schematic representation of the *sef* gene locus. Putative annotations are as follows: CHASE2 extracellular sensory domain and guanylate cyclase (with sec leader peptide in red); TPR, tetratricopeptide repeat containing protein; SefA, selenium nanosphere assembly protein; SefB, SAM-methyltransferase; ? putative peptide; DUF, domain of unknown function. The (B) nucleotide sequence of the promoter region of *sefA*. (C) nucleotide sequence upstream from *sefB*. A putative Shine–Dalgarno (SD) sequence and putative Fnr_{Bac}/PrfA binding motif (TGTGA –N₆-TCACA) are located upstream of *sefA*. No obvious promoter binding sequences are identified between *sefA* and *sefB*. A putative SD sequence upstream of *sefB* is also located.

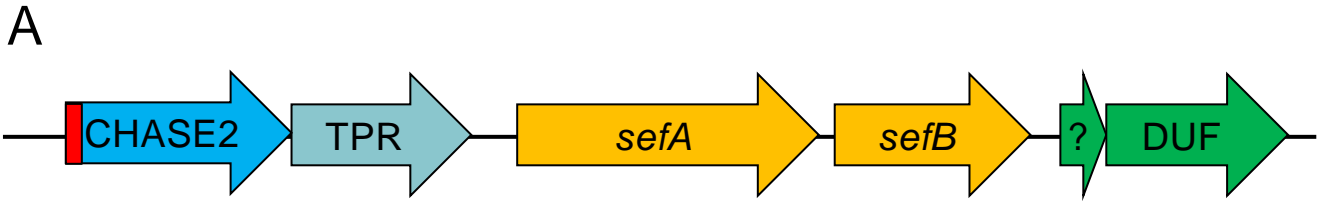
Fig. 4. Expression of SefA in *E. coli* and *in vitro* formation of Se-nanospheres. (A) Western blot analysis of the localisation of SefA expression in *E. coli* following exposure to selenite. Samples (10 μ g) were prepared from cells +/- IPTG and +/- selenite (10 mM). Lanes (2,4,6) represent extracellular protein; Lanes (3,5,7) represent soluble cell extracts. Samples were analysed at both 4h and 19h post the addition of IPTG and selenite. Lanes 1 and 8 show an 80 kDa marker. (B) TE micrograph of an *E. coli* single cell harbouring

plasmid pET33b-*sefA* grown in the presence of selenite (10 mM), but not induced with IPTG. (C) TE micrograph of an *E. coli* single cell harbouring plasmid pET33b-*sefA* grown in the presence of both selenite (10 mM) and IPTG. Three replicate cells are shown in Fig S3. Selenium deposits are indicated by an arrow. (D) Growth yield at stationary phase of *E. coli* cells exposed to increasing selenite concentrations. *E. coli* harbouring plasmid pET33b-*sefA* in the absence (hashed bars) or presence (solid bars) of IPTG and *E. coli* cells harbouring plasmid pET33b in the presence of IPTG (open bars). Error bars are SEM ($n = 3$). ** indicates *T*-test, $p < 0.01$ compared to the non-recombinant (pET33b) control. (E) The reaction of GSH (4 mM) with selenite (0.5 mM), either in the presence (○) or absence (■) of purified rSefA (0.5 μg), monitored at 400 nm. TE micrographs of the reaction product from (E), in the absence (F) and in the presence (G) of SefA. Scale bars are 0.5 μm and 200 nm for C and D, respectively.

Fig. 5. Schematic diagram showing the proposed pathway of selenium oxyanion reduction and Se-nanosphere assembly in *T. selenatis*. The reduction of selenate draws electrons from the membrane-bound QCR, generating a net gain of $2q^+/2e^-$ of proton electrochemical gradient which could provide the driving force for the translocation of selenite across the cytoplasmic membrane. Once in the cytoplasm, selenite reduction occurs and the resultant Se^0 binds to SefA forming a Se-nanosphere prior to export from the cell. Process by which SefA-Se is exported remains unknown. The identification of a gene (*sefB*) encoding a putative SAM-dependent methyltransferase might also provide a mechanism for selenite detoxification via volatilisation to methylated selenides (R-Se-R). OM represents the outer membrane. IM represents the cytoplasmic inner membrane.







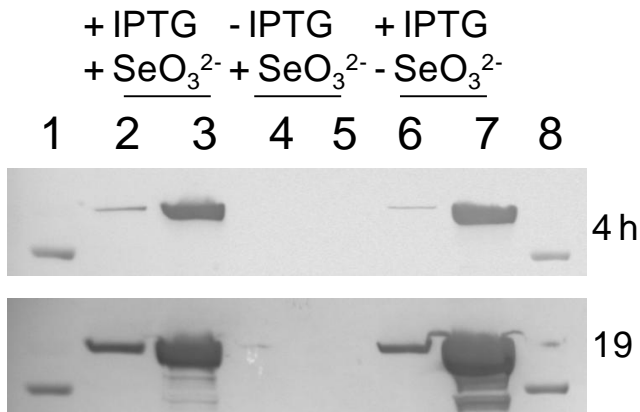
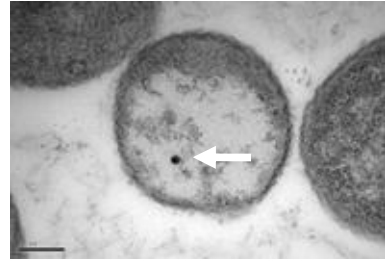
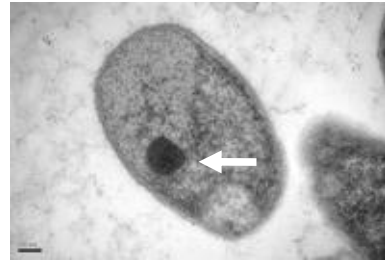
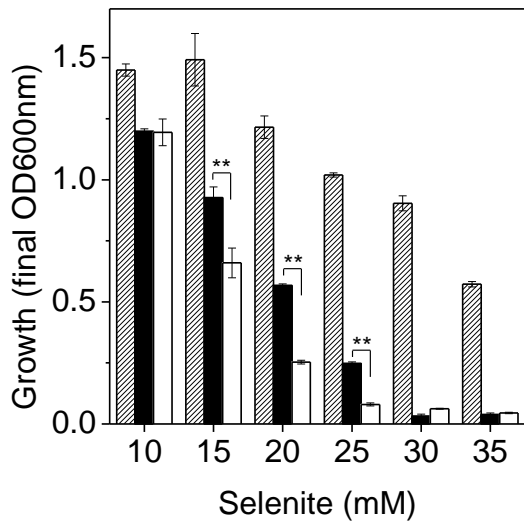
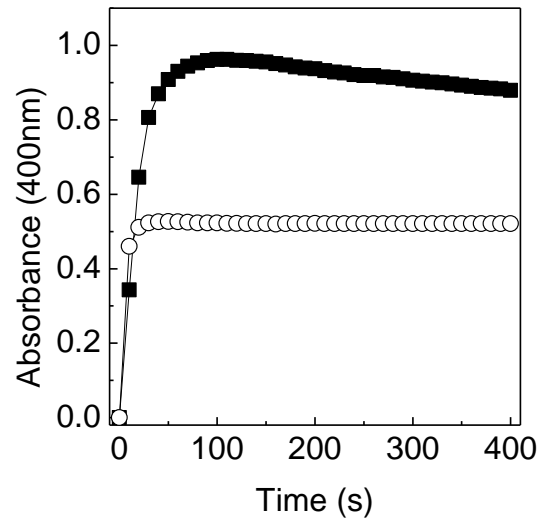
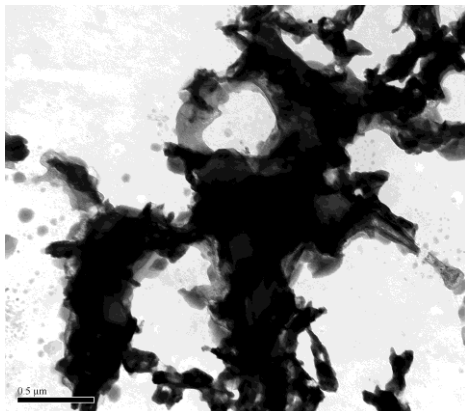
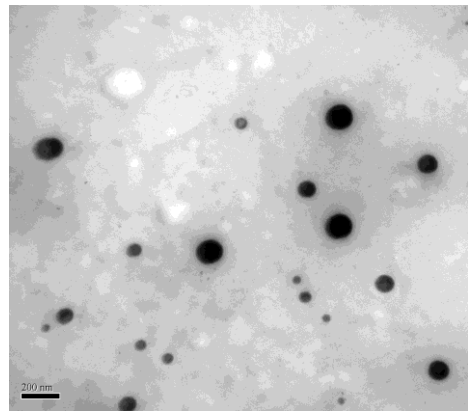
B

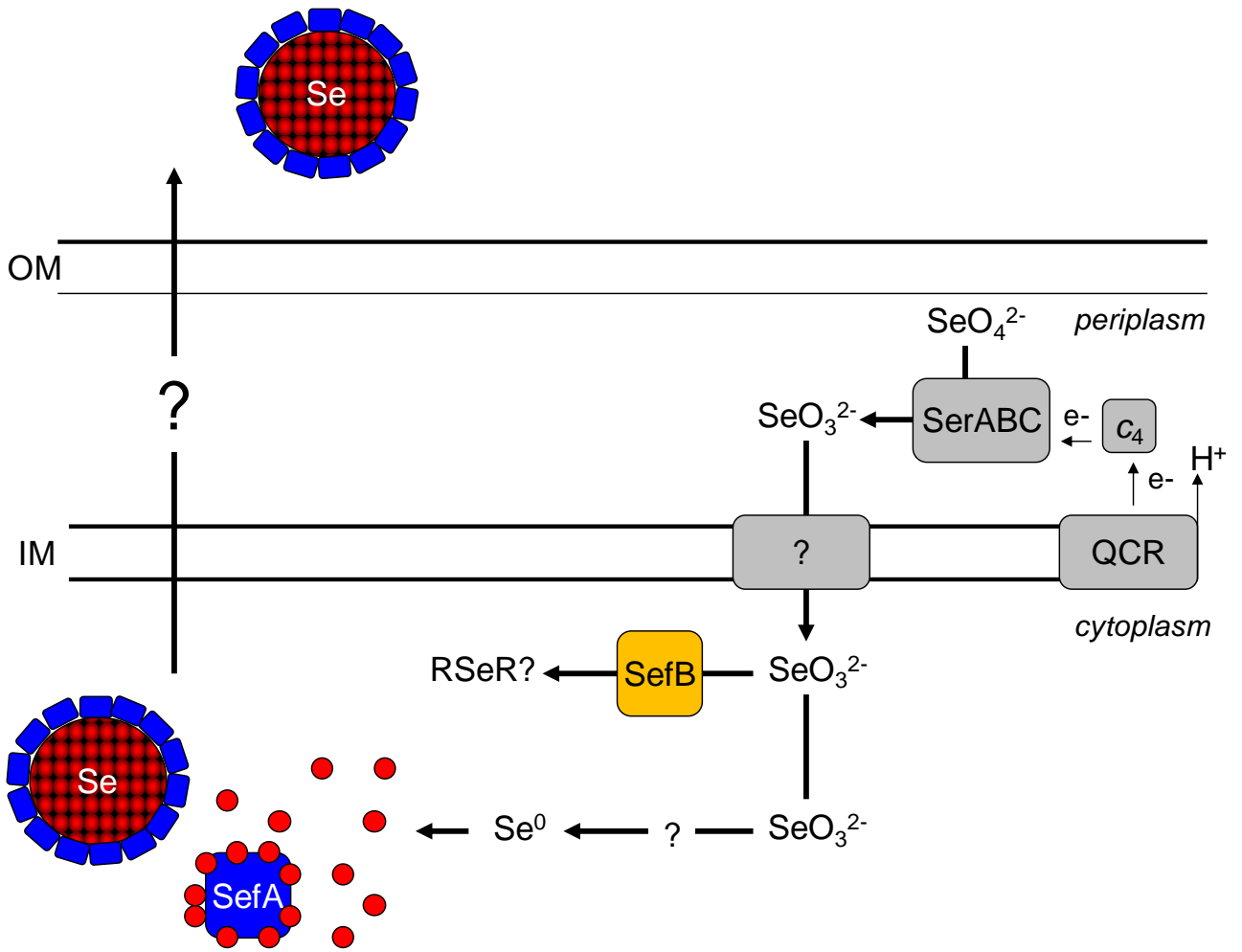
5' - TACTTCGGCGCCCGATATCGCCACTAGCGCACGTATCG
 CGTAGACGCGCGTTGTTTTTTTTGCTACAGCCGTGGCTC
GTGTGATTCCCATCACATCGCTTGCCCCGACTTTCATT
 Fnr_{Bac}/PrfA
 AA ACTGCGATTTCGCGTTTCAGGGCCCGCGAGGGTCGAA

TCCCTTTTTCCACCAGGAGATGCTTCAC|ATGGCTATCA - 3'
 SD M A I → SefA

C

5' - TAATCGCCTACCGCGATCCTCTCGTCCGCAAGGGCGAG
 AGGACAGGCTCTACAACCCCGCCTCCTGAAAAGGGGGT
 GGGTTTTTTCTTGTGGTGTGGGGATCTCGACATCACC
 AGAAAAACCTCACCGAATTGAATAGAAAGGAATACCC
 SD
 ATTATGAGTGAC - 3'
 M S D → SefB

A**B****C****D****E****F****G**



Supporting Information

SI Materials and Methods

Growth of *T. selenatis* and *E. coli*. *T. selenatis* was cultured anaerobically (at 30°C) on mineral salts medium containing yeast extract (0.1%), with either selenate or nitrite (10 mM) as terminal electron acceptors and acetate (10 mM) as the electron donor in 1 L batch cultures. Cultures were also grown under aerobic conditions on Luria-Bertani (LB) medium supplemented with selenate, selenite or nitrate (all at 10 mM unless otherwise indicated). All *E. coli* cultures were grown on LB medium at 37°C.

Isolation of SefA. Cultures were harvested during late log phase (after 16-18 hours growth) at OD_{600nm} 0.6-0.7 by centrifugation (25,000 x g, 20 minutes) and the supernatant, containing the Se-nanospheres and extra-cellular media, was retained. The supernatant was passed through a 0.2 µm filter, to remove bacterial cells, and concentrated using an Amicon ultra centrifugation filtrate unit with a 10 kDa cut off (Millipore). Isolated extracellular protein was analysed by SDS-PAGE. Protein samples were tested for selenite reductase activity as described by Ridley *et al.* (1).

Identification of the *sefA* gene. Isolated SefA was resolved by SDS-PAGE, excised and sent for N-terminal sequencing at Pinnacle Proteomic facility, Newcastle University. In addition, gel slices containing SefA were sent to Mass Spectrometry facilities at the Universities of Exeter and York. To identify the *sefA* gene the protein sequencing data obtained was blasted against the draft genome sequence of *T. selenatis* (10) using CLC genomics work bench 3 gene prediction software.

Generation of recombinant SefA. The coding region of SefA was amplified using forward (5'-GTTCATATGGCTATCACTGCG ACTCAACGC-3', underlined sequence *NdeI* restriction site) and reverse (5'-GGACTCGAG TTAGAACAGGTAGATGTTGCC -3', underlined sequence *XhoI* restriction site) primers and cloned into pET33b(+) using *NdeI* and *XhoI* restriction sites. Insertion of *sefA* into pET33b(+) using these restriction sites inserted a N terminal 6 X His-tag (His-SefA). The plasmid was designated pET33b-*sefA*. Cloning of *sefA* was confirmed by analytical restriction digestion and DNA sequencing. SefA was overexpressed in *E. coli* BL21 CodonPlus (DE3) – RIPL cells and purified by immobilized metal affinity chromatography in buffer A (20 mM Tris-HCl pH 8.0, 0.5 M NaCl) and gel filtration. Extracellular proteins were concentrated from 50 ml culture to 1 ml samples using U-Tube 20-30 concentrators (Novagen). Samples were resolved by SDS-PAGE and Western blotting was used to detect His-tagged protein to determine localisation. Immuno-cross-reactive proteins were detected using 1' monoclonal anti-polyHistidine antibody (Sigma) and 2' anti-mouse IgG (H+L) AP conjugate (Promega). The samples were detected by the addition of Western blue stabilized substrate for alkaline phosphatase (Promega).

***In vitro* formation of selenium nanospheres.** Selenium nanoparticle formation assays were performed in 50 mM Tris-HCl buffer (pH 7.0) supplemented with protein, 4 mM reduced glutathione and 0.5 mM selenite at room temperature in quartz cuvettes (2). The formation of selenium nanospheres was monitored spectrometrically at 400 nm. All solutions were sparged with nitrogen before use.

Imaging Se-nanospheres by Transmission Electron Microscopy (TEM). *T. selenatis* and *E. coli* cultures were centrifuged at 6000 x g for 3 minutes in a 50 ml falcon tube, supernatant removed and a fixative of 2% (w/v) paraformaldehyde, 2.5% (v/v) glutaraldehyde in 0.1M cacodylate buffer pH 7.2 was added. Fixation time was a minimum of 2 hours. Post fixation was carried out with 1% (v/v) osmium tetroxide in 0.1M cacodylate buffer pH 7.2 followed by embedding in 3% (w/v) agarose LM in 0.1M cacodylate buffer pH 7.2. After cooling on ice the plug of agar was removed and cut into 3 mm² pieces, washed, stained with 1% (w/v) uranyl acetate for 1 h, washed and dehydrated. After embedding in TAAB Low Viscosity Resin Hard (TAAB Laboratories Equipment Ltd, Berkshire, UK), sections of 80-90 µm thickness were cut with a diamond knife and collected on carbon-coated Formvar films on 300-mesh copper grids. Sections were stained with uranyl acetate and lead citrate before being examined at 80 kV with a Jeol 1400 transmission electron microscope. For *in vitro* generated selenium particles, droplets of sample were placed on carbon-coated Formvar films on 300 mesh copper grids for 1 min, after which excess liquid was withdrawn with filter paper. Grids were placed on filter paper and air-dried. Specimens examined at 80 kV or 100 kV with a Jeol 1400 transmission electron microscope.

RNA isolation. For transcriptional studies, bacteria were grown aerobically at 30°C in LB broth supplemented with various concentrations of selenite. Total RNA was extracted from 10 ml of exponentially growing cultures (OD_{600 nm} of 1) and 5 ml of stationary phase cultures at 16 hrs after inoculation, respectively, using a hot-phenol extraction protocol (3). In brief, cells were harvested by centrifugation at 4,000 rpm at 4°C for 10 mins. The cell pellet was resuspended in 1 ml of ice-cold resuspension buffer (10 mM KCl, 5 mM MgCl₂, 10 mM Tris; pH 7.4) and 0.5 ml each were added to pre-heated tubes containing 0.4 ml of lysis buffer (0.4 M NaCl, 40 mM EDTA, 1% 3-mercaptoethanol, 1% sodium dodecyl sulfate, 20 mM Tris; pH 7.4) and 0.2 ml of acid phenol (pH 4.5; Ambion), using duplicate tubes per sample. The tubes were incubated at 90°C for 5 mins and then chilled on ice for 5 mins. Phase separation was achieved by centrifugation at 13,000 rpm for 2 mins. RNA in the supernatant was extracted with two additional phenol-chloroform extraction and precipitated over night at -20°C in isopropanol. The RNA was pelleted by centrifugation, washed with 70% ethanol, air dried for 5 mins at room temperature and resuspended in nuclease-free water. Contaminating DNA was removed by DNase I (Ambion) digestion for 45 mins at 37°C, followed by phenol/chloroform extractions, isopropanol precipitation and resuspension of the total RNA in nuclease-free water as described above.

Reverse transcription-PCR (RT-PCR). For cDNA synthesis, 4 µg of total RNA was mixed with 3 µl of random primers at 3 µg/µl (Invitrogen) and 1 µl of a dNTP mixture at 10 mM each (Promega). After primer annealing at 65°C for 5 mins, a mix of first-strand buffer, DTT, 40 U RNase OUT recombinant RNase inhibitor (Invitrogen), and 200 U Superscript III reverse transcriptase (Invitrogen) was added according to the manufacturer's recommendations. cDNA synthesis was performed at 50°C for 60 min, followed by heat inactivation at 70°C for 15 min. cDNA samples were 10x diluted in water and directly used for PCR amplification. *sefA* transcript levels were determined using primers *sef-fw* (CGACTCGAGGGCACCTTCGGTACTGTAAC) and *sef-rv* (CGCTCTAGACGGAGGTCAGCAGATCATTC). For the adjustment of cDNA amounts, 16S rRNA was used as an internal standard, using primers Ts-16S-RT-1 (GCAGTGAAATGCGTAGAG) and Ts-16S-RT-2

(TGTC AAGGGTAGGTAAGG) for the PCR reaction. As a control for DNA contaminations, PCRs were performed using total RNA without any reverse transcription reaction.

Northern Blot. For northern blotting, 5 µg of total RNA was separated on a 1.5 % formaldehyde agarose gel prior to blotting onto a Hybond-N⁺ membrane by capillary transfer. The *sefA* transcript was detected by hybridizing the membrane with a DIG-labeled DNA probe at 50°C over night. For amplification of the probe, the PCR DIG probe synthesis kit (Roche) was used with primers *sef-fw* and *sef-rv* (see above). The membrane was developed using an anti-digoxigenin antibody and CDP-Star substrate (Roche) according to the manufacturer's recommendations. Chemiluminescent signals were visualized and quantified using a Chemidoc XRS system equipped with the QuantityOne software (BioRad).

References:

1. Ridley H, Watts CA, Richardson DJ, Butler CS (2006) Development of a viologen based microtitre plate assay for the analysis of oxyanion reductase activity: Application to the membrane bound selenate reductase from *Enterobacter cloacae* SLD1a-1. *Anal Biochem* 358:289-294
2. Kessi J, Hanselmann KW (2004) Similarities between the abiotic reduction of selenite with glutathione and the dissimilatory reaction mediated by *Rhodospirillum rubrum* and *Escherichia coli*. *J Biol Chem* 279:50662-50669.
3. Chuang SE, Daniels DL, Blattner FR (1993) Global regulation of gene expression in *Escherichia coli*. *J. Bacteriol.* 175:2026-2036.

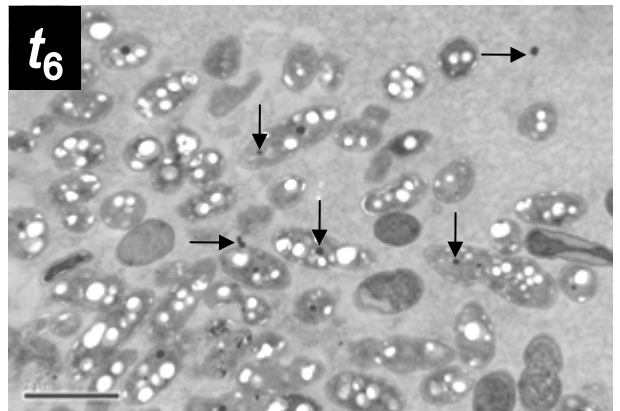
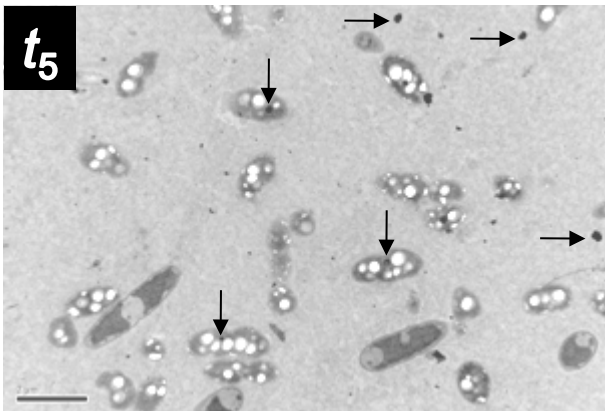
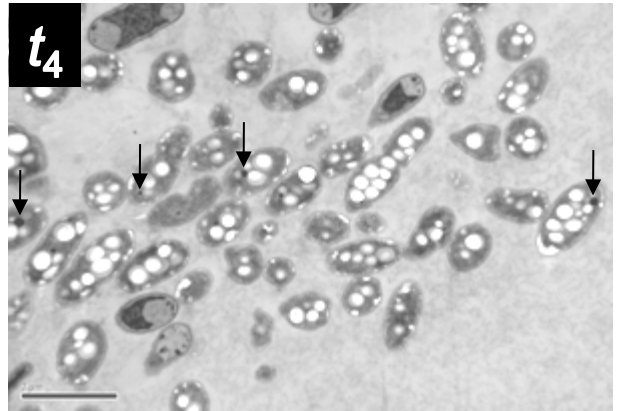
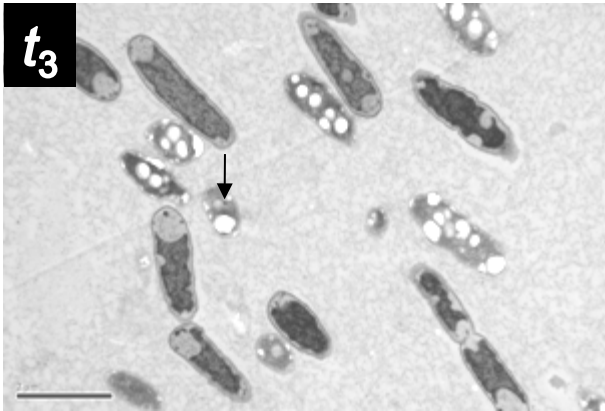
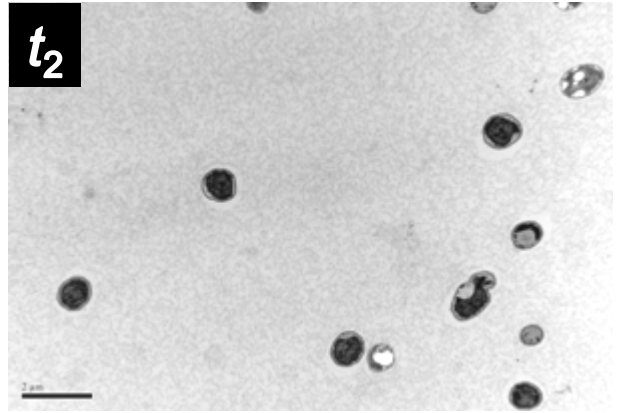
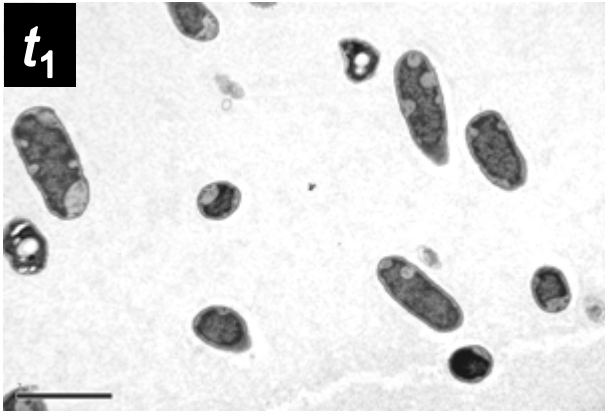
SI Figure legends

Fig. S1. Transmission electron micrographs of *T. selenatis* cells grown under selenate respiration conditions show the formation of selenium deposits. Images show cell cohorts to indicate the distribution of typical cells shown in Fig. 1. Micrographs t_1 and t_2 show mid exponential phase; t_3 and t_4 show late exponential phase; t_5 and t_6 show stationary phase. Scale bar = 2 µm in each case. Intracellular Se-deposits are indicated by a vertical arrow. Extracellular Se-deposits are indicated by a horizontal arrow.

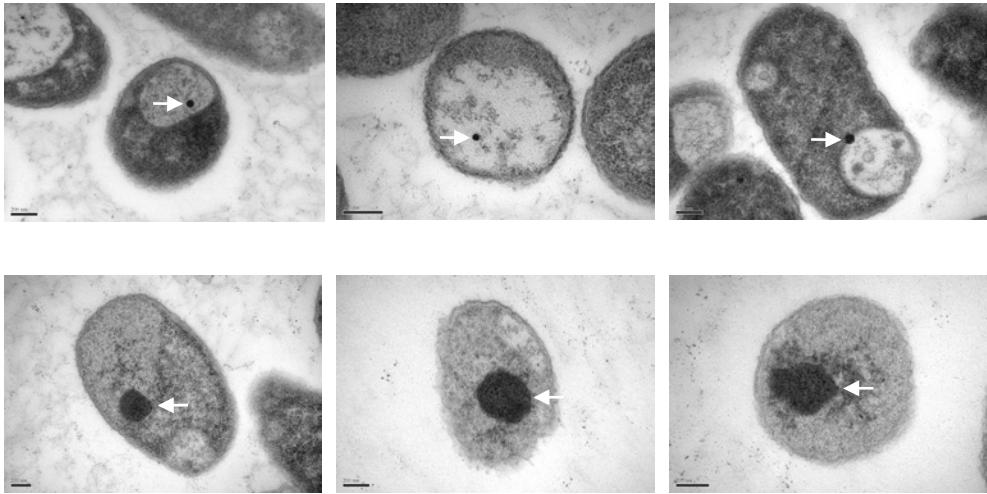
Fig. S2. Alignment of SefA with a hypothetical protein (NAL212_3002) from *Nitrosomonas* sp. AL212. Residues in *red* indicate the peptide determined by N-terminal sequencing of the mature peptide secreted from *T. selenatis*. Residues in *green* indicate the peptides generated during tryptic digest for MS analysis. Sequence in *blue* indicates the glycine rich repeat (GGXGXDXXX) associated with TISS substrates. Alignment performed using ClustalW2.

Fig. S3. Expression and purification of SefA from *E. coli*. Transmission electron micrographs of *E. coli* single cells harbouring plasmid pET33b-*sefA* grown in the presence of selenite (10 mM), but not induced with IPTG. (*upper pannel*). TE micrographs of *E. coli* single cells harbouring plasmid pET33b-*sefA* grown in the presence of both selenite (10 mM) and IPTG (*lower panel*). Three replicate cells are shown. (*B*) SDS-PAGE analysis of SefA expression in *E. coli*. Lane 1, molecular weight markers; lane 2, purified SefA secreted from *T. selenatis*; lane 3, extracellular protein from non-induced cells; lane 4, extracellular protein from induced cells; lane 5

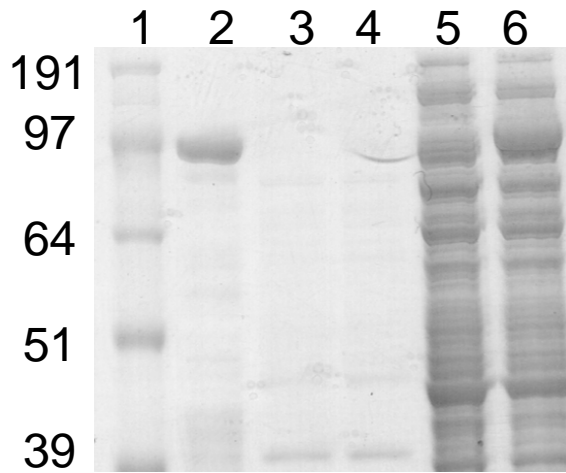
soluble cell extracts from non-induced cells; lane 6, soluble cell extracts from induced cells. (C) Purification of SefA from *E. coli* following induction with IPTG. Lane 1, molecular weight marker; lane 2, purified SefA secreted from *T. selenatis*; lane 3, total soluble protein; lane 4, flow through from nickel column; lane 5, wash through; lane 6, wash with 20 mM imidazole buffer; lane 7, elution with 250 mM imidazole buffer; lane 8, purified SefA post gel-filtration.



A



B



C

